A Wavelet Based Adaptive Discontinuous Galerkin Method for Incompressible Flows

Brijesh Pinto, Marta de la Llave Plata and Eric Lamballais

Abstract This paper outlines the development of a wavelet based adaptive discontinuous Galerkin spectral element method (DG-SEM) for unsteady incompressible flows. The proposed approach possesses arbitrary high formal accuracy and permits adaptivity in a way that is computationally cheap and efficient. An element wise discretisation of the domain is performed. Two sets of basis functions are employed per element—the Lagrange polynomials at the Gauss-Legendre-Lobatto (GLL) points which acts as the nodal basis for the DG-SEM method and the second generation wavelets (SGW) which can be looked upon as either a nodal or modal basis, subject to convenience, and is responsible for facilitating the adaptivity. The projection of the signal onto the wavelet space provides information about the local frequency content of the signal. An accumulation of high frequency components acts as an indicator for dynamic mesh refinement via thresholding. The main advantage of using the SGW basis is the low cost of the transform, *O(N)* per direction.

1 Introduction

High-order simulations of unsteady incompressible turbulent flows are very challenging, especially at high Reynolds numbers (Re) and in complex geometries. Grid resolution scales as $\frac{\eta}{L} = \left(\frac{1}{Re}\right)^{\frac{9}{4}}$, thus at high Re, the large grid sizes required, make

B. Pinto (✉) · M. de la Llave Plata
ONERA, 92322 Châtillon, France
e-mail: brijesh_emmanuel.pinto@onera.fr

M. de la Llave Plata
e-mail: marta.de_la_llave_plata@onera.fr

E. Lamballais
Laboratoire d'Etudes Aérodynamiques, UMR 6609 Université de Poitiers, CNRS,
Téléport 2 - Bd. Marie et Pierre Curie, B.P. 30179, 86962 Futuroscope Chasseneuil Cedex, France
e-mail: eric.lamballais@univ-poitiers.fr

M.O. Deville et al. (eds.), *Turbulence and Interactions*,
Notes on Numerical Fluid Mechanics and Multidisciplinary Design 135,
https://doi.org/10.1007/978-3-319-60387-2_22

DNS infeasible. A way to overcome this problem is via large eddy simulation (LES) and *hp*-adaptivity. Both these techniques require the usage of efficient high-order discretization schemes. In response to this requirement we are working on the development of high-order, *hp*-adaptive incompressible flow solvers for DNS and LES. In general, modern solver methods should possess several beneficial properties such as high formal order of accuracy, relatively low operation count and good parallel performance.

Spectral methods (SM) and spectral element methods (SEM) using continuous Galerkin (CG) [1] have seen widespread use for fluid flow problems, albeit on simple geometries. Although they possess remarkable accuracy, their principal failing is their instability in convection dominated flows. The discontinuous Galerkin spectral element method (DG-SEM) is a variant of SEM employing a non-conforming approximation space [2], leading to superior performance in the convection dominated regime. In addition, DG-SEM also possesses a a compact stencil, important for parallel computations wherein interprocess passes are sought to be kept to a minimum [3]. However as a general rule spectral methods are computationally expensive. *hp*-adaptivity seeks to overcome this problem via concentrating computational resources where they are most needed. However typically adaptivity necessitates an error estimator or refinement indicator to highlight those regions in the flow where refinement is needed. For unsteady incompressible flows there is a severe deficiency of suitable error estimators. The usage of wavelets for adaptivity and LES in incompressible flows has a rich history [4]. Thus we intend to use second generation wavelets (SGW) as a refinement indicator. The multi-resolution analysis (MRA) (constructed using SGW) of the flow field gives us information regarding the signal regularity. A local loss in regularity indicates the need for *hp*-refinement. Here we utilize SGW in conjunction with DG-SEM for incompressible flows. Recent work along similar lines, albeit in the compressible flow regime [5] lends credence to this approach. In this paper we first describe the variant of DG-SEM method which we use. Next we describe the wavelet basis and its applications to adaptivity. We conclude with some results.

2 Discontinuous Galerkin Method for Incompressible Flows

The incompressible Navier–Stokes equations are given as:

$$\begin{aligned} \partial_t \mathbf{u} - \nu \triangle \mathbf{u} + \nabla . \mathscr{F}(\mathbf{u}) + \nabla p = f \;\; in \;\; \Omega, \;\; t \;\; \varepsilon \;\; [0,T] \\ \nabla . \mathbf{u} = 0 \;\; in \;\; \Omega, \;\; t \;\; \varepsilon \;\; [0,T] \\ \mathbf{u} = \mathbf{g} \;\; on \;\; \partial\Omega_g, \;\; t \;\; \varepsilon \;\; [0,T] \\ (\nu \nabla \mathbf{u}) . \hat{n} = \mathbf{h} \;\; on \;\; \partial\Omega_h, \;\; t \;\; \varepsilon \;\; [0,T] \end{aligned} \tag{1}$$

where $\mathscr{F}(\mathbf{u}) = (\mathbf{u} \otimes \mathbf{u})$. Over the last decade there has been a proliferation of discretization techniques based on non-conforming approximation spaces. We have chosen a local discontinuous Galerkin (LDG) discretization strategy which uses $Q_k - Q_k$ velocity-pressure approximation space (equal order) and pressure-jump stabilization for satisfaction of the *inf-sup* condition [2, 6, 7]. Such a method ensures the satisfaction of *inf-sup* condition independent of the grid. It also offers the additional benefit of allowing all velocity components and pressure to be hosted at the same element node in a nodal DG setting, greatly simplifying the construction of the code and removing the need for costly interpolations. This property also dovetails rather nicely with the SGW transform which acts upon the element degrees of freedom as will be seen in Sect. 3.

We briefly present the details of the LDG discretisation. The domain (Ω) is first partitioned into elements $\Omega = \bigcup_j \mathbf{T}_j$. The collection of these element forms the mesh $\mathbb{T} = \{\mathbf{T}\}$. The boundaries of the domain are denoted as $\partial\Omega$ while element boundaries are denoted by $\partial\mathbf{T}$. Let $\mathbf{T}_1$ and $\mathbf{T}_2$ be two adjacent elements. We define an *interface* as $F^i = \partial\mathbf{T}_1 \cap \partial\mathbf{T}_2$. Similarly a *boundary face* is defined by $F^b = \partial\mathbf{T} \cap \partial\Omega$. The set of all faces is defined by $\mathbb{F} = \{F^i \cup F^b\}$. Each face has an associated length scale denoted as $h_{\mathbf{F}}$.

At the faces, the following definitions are needed. Let u be a piecewise-smooth scalar variable. The trace of u along the *interface* of two elements $\mathbf{T}_1$ and $\mathbf{T}_2$ is denoted as $u|_{\partial\mathbf{T}_1}$ and $u|_{\partial\mathbf{T}_2}$ respectively. Then $[\![u]\!] = (u|_{\partial\mathbf{T}_1} - u|_{\partial\mathbf{T}_2})$ represent the *jump* across the interface. Furthermore $\{\{u\}\} = \frac{1}{2}(u|_{\partial\mathbf{T}_1} + u|_{\partial\mathbf{T}_2})$ represents the *average* along the *interface*. For a piecewise-smooth vector variable $\mathbf{u}$ we can define a jump across the *interface* as $[\![\mathbf{u}]\!] = (\mathbf{u}|_{\partial\mathbf{T}_1}.\hat{n} - \mathbf{u}|_{\partial\mathbf{T}_2}.\hat{n})$, where $\hat{n}$ is the unit normal to the interface, while the average is defined as $\{\{\mathbf{u}\}\} = \frac{1}{2}(\mathbf{u}|_{\partial\mathbf{T}_1}.\hat{n} + \mathbf{u}|_{\partial\mathbf{T}_2}.\hat{n})$.

We equip each element with an appropriate local polynomial space, of maximum degree k in each variable, denoted as $Q_k(\mathbf{T})$. Then we define the following broken polynomial spaces for velocity and pressure:

$$V_h(\mathbb{T}) = \{\mathbf{v}\ \varepsilon\ [L^2(\Omega)]^d \mid \mathbf{v}|_{\mathbf{T}}\ \varepsilon\ [Q_k]^d(\mathbf{T}),\ \forall\ \mathbf{T}\ \varepsilon\ \mathbb{T}\}$$
$$Q_h(\mathbb{T}) = \{q\ \varepsilon\ L^2(\Omega) \mid q|_{\mathbf{T}}\ \varepsilon\ Q_k(\mathbf{T}),\ \forall\ \mathbf{T}\ \varepsilon\ \mathbb{T}\}$$

where d is the dimension. Thus the weak form of the LDG discretisation of Eq. 1 is given as: $\{\mathbf{u}_h, p_h\}\ \varepsilon\ \{V_h, Q_h\}$ such that

$$\partial_t(\mathbf{v}_h, \mathbf{u}_h) + \nu a_h^{sip}(\mathbf{v}_h, \mathbf{u}_h) + \mathscr{A}_h^{nl}(\mathbf{v}_h, \mathbf{u}_h) + b_h(p_h, \mathbf{v}_h) - b_h(q_h, \mathbf{u}_h) + s_h(q_h, p_h) = (\mathbf{v}_h, f) + G_h(\mathbf{v}_h) \tag{2}$$

is satisfied $\forall\{\mathbf{v}_h, q_h\}\ \varepsilon\ \{V_h, Q_h\}$. In Eq. 2, a_h^{sip} represents the symmetric interior penalty (SIP) bilinear form of the viscous term, given by:

$$a_h^{sip}(\mathbf{v}_h, \mathbf{u}_h) = \sum_{\mathbf{T}\varepsilon\mathbb{T}} \int_{\mathbf{T}} \nabla_h \mathbf{v}_h : \nabla_h \mathbf{u}_h d\mathbf{x} - \sum_{\mathbf{F}\varepsilon\mathbb{F}} \int_{\mathbf{F}} \{\{(\nabla_h \mathbf{u}_h).\hat{n}\}\}.[\![\mathbf{v}_h]\!] d\mathbf{s}$$
$$- \sum_{\mathbf{F}\varepsilon\mathbb{F}} \int_{\mathbf{F}} \{\{(\nabla_h \mathbf{v}_h).\hat{n}\}\}.[\![\mathbf{u}_h]\!] d\mathbf{s} + \sum_{\mathbf{F}\varepsilon\mathbb{F}} \frac{\eta}{h_{\mathbf{F}}} \int_{\mathbf{F}} [\![\mathbf{v}_h]\!].[\![\mathbf{u}_h]\!] d\mathbf{s}$$

where η represents the penalty parameter. $\mathscr{A}_h^{nl}(\mathbf{v}_h, \mathbf{u}_h)$ represents the weak form of the non-linear term, given by:

$$\mathscr{A}^{nl}(\mathbf{v}_h, \mathbf{u}_h) = -\sum_{\mathbf{T}\varepsilon\mathbb{T}} \int_{\mathbf{T}} \nabla_h \mathbf{v}_h : \mathscr{F}(\mathbf{u}_h) d\mathbf{x} + \sum_{\mathbf{F}\varepsilon\mathbb{F}} \int_{\partial T} \mathscr{F}^N(\mathbf{u}_h^+, \mathbf{u}_h^-).[\![\mathbf{v}_h]\!] d\mathbf{s}$$

with $\mathscr{F}^N(\mathbf{u}_h^+, \mathbf{u}_h^-)$ as a central numerical flux given by:

$$\mathscr{F}^N(\mathbf{u}_h) = \frac{\mathscr{F}(\mathbf{u}_h^-).\hat{n} + \mathscr{F}(\mathbf{u}_h^+).\hat{n}}{2}$$

and:

$$\mathbf{u}_h^- = \begin{cases} \mathbf{u}_h|_{\partial\mathbf{T}_1} \; in \;\; \mathbf{F} \; \varepsilon \; F^i \\ \mathbf{u}_h|_{\partial\mathbf{T}} \; in \;\; \mathbf{F} \; \varepsilon \; F_g^b \end{cases} \qquad \mathbf{u}_h^+ = \begin{cases} \mathbf{u}_h|_{\partial\mathbf{T}_2} \; in \;\; \mathbf{F} \; \varepsilon \; F^i \\ \mathbf{g} \quad\;\; in \;\; \mathbf{F} \; \varepsilon \; F_g^b \end{cases}$$

In Eq. 2, b_h is the bilinear form for the pressure and divergence operators given by:

$$b_h^{div}(\mathbf{v}_h, q_h) = \sum_{\mathbf{T}\in\mathbb{T}} \int_{\mathbf{T}} \mathbf{v}_h.\nabla_h q_h d\mathbf{x} - \sum_{\mathbf{F}\in F^i} \int_{\mathbf{F}} \{\{\mathbf{v}_h.\hat{n}\}\}[\![q_h]\!] d\mathbf{s}$$

$S_h(q_h, p_h)$ is the pressure-jump stabilization bilinear form given by:

$$S_h(q_h, p_h) = \sum_{\mathbf{F}\varepsilon\mathbb{F}^i} \frac{h_{\mathbf{F}}}{\nu} \int_{\mathbf{F}} [\![q_h]\!][\![p_h]\!] d\mathbf{s}$$

and finally $G_h(\mathbf{v}_h)$, containing the boundary terms, is given by:

$$G_h(\mathbf{v}_h) = \sum_{\mathbf{F}\varepsilon F_h^b} \int_{\mathbf{F}} \mathbf{v}_h.\mathbf{h} d\mathbf{s} - \sum_{\mathbf{F}\varepsilon F_g^b} \int_{\mathbf{F}} \left(\nu \; \mathbf{g}.(\nabla_h \mathbf{v}_h).\hat{n} + \nu \; \frac{\eta}{h_{\mathbf{F}}} \mathbf{v}_h.\mathbf{g} + q_h \mathbf{g}.\hat{n}\right) d\mathbf{s}$$

The temporal discretisation is performed via classical second order pressure correction techniques detailed in [2, 8].

3 Second Generation Wavelets (SGW), Multi-resolution Analysis (MRA) and Adaptivity

In principle the decay of coefficients of an approximating polynomial series is linked directly to the regularity of the target function. As an example, the projection of a target function onto a Fourier basis provides data about which frequencies contribute the most energy. However modal bases (like Fourier) are typically well localized in frequency space and poorly localized in physical space, making it impossible to determine where in space to refine to better capture the signal.

A solution to this problem is to use a wavelet basis, one which is well localized in both space and frequency. Wavelet bases may be used to construct a hierarchy of space-frequency windows each with its own space-frequency range. This construction is called a *multi-resolution analysis* (MRA). By projecting a target function upon an MRA and by then examining the coefficients within each space-frequency tile we can refine in exactly the correct spatial location as the signal demands. In this work we will use a *second generation wavelet* (SGW) basis [9], one which can be built directly in physical space and upon bounded domains.

The MRA denoted by $\mathbf{M}$, is the partitioning of the function space $L^2(R)$, by a sequence of nested closed subspaces V_j, called *scaling function space*, such that $\mathbf{M} = \{V_j \subset L^2(R) \mid j \; \varepsilon \; \mathbb{J} \subset Z\}$. This set of subspaces must satisfy the following properties:

1. Nestedness of spaces:

$$V_{-\infty} \subset ...V_{-2} \subset V_{-1} \subset V_0 \subset V_1 \subset V_2 ... \subset V_j \subset V_{j+1} \subset ...V_{+\infty} \quad j \; \varepsilon \; Z$$

   with resolution increasing towards continuum as $j \to \infty$.
2. Closure of $L^2(R)$:

$$\overline{\bigcup_j V_j} = L^2(R) \quad j \; \varepsilon \; Z$$

3. For each $j \; \varepsilon \; \mathbb{J}$, V_j has a Riesz basis given by *scaling functions* $\{\phi_k^j \mid k \; \varepsilon \; \mathbb{K}(j)\}$. $\mathbb{K}(j)$ is an index set such that $\mathbb{K}(j) \subset \mathbb{K}(j+1)$. We may consider two cases for the index set $\mathbb{J}$:
   a. $\mathbb{J} = N$. In such a case the coarsest level exists and is V_0.
   b. $\mathbb{J} = Z$. This is a bi-infinite setting.

We now define the *wavelet space*, denoted by W_j. A set of functions $\{\psi_m^j \mid j \; \varepsilon \; \mathbb{J}, \; m \; \varepsilon \; \mathbb{M}(j) \mid \mathbb{M}(j) = \mathbb{K}(j+1)/\mathbb{K}(j)\}$, are the basis functions of the space W_j and are called *wavelets*. The *wavelets* and the spaces which they span must satisfy the following properties:

1. The space W_j is the complement space of V_j in V_{j+1} i.e. $V_{j+1} = V_j \oplus W_j$
2. The wavelet space is complete:

$$\overline{\bigcup_j W_j} = L^2(R) \quad j \; \varepsilon \; Z$$

3. a. if $\mathbb{J} = N$. Then the set $\{\psi_m^j / ||\psi_m^j||, \; j \; \varepsilon \; \mathbb{J}, \; m \; \varepsilon \; \mathbb{M}(j)\} \bigcup \{\phi_k^0 / ||\phi_k^0||, \; k \; \varepsilon \; \mathbb{K}(0)\}$ is a Riesz basis for $L^2(R)$
   b. if $\mathbb{J} = Z$. Then the set $\{\psi_m^j / ||\psi_m^j||, \; j \; \varepsilon \; \mathbb{J}, \; m \; \varepsilon \; \mathbb{M}(j)\}$ is a Riesz basis for $L^2(R)$

We now define the *dual* MRA $\tilde{\mathbf{M}} = \{\tilde{V}_j \subset L^2(R) \mid j \; \varepsilon \; \mathbb{J} \subset Z\}$. The space $\tilde{V}_j$ is termed as *dual scaling function space* and it is spanned by the *dual scaling functions* denoted as $\tilde{\phi}_k^j$. Similarly we define a *dual wavelet space* denoted by $\tilde{W}_j$ with basis functions as *dual wavelets* denoted as $\tilde{\psi}_m^j$. The space $\tilde{W}_j$ is the complement to the space $\tilde{V}_j$.

Consider a function $f(x) \; \varepsilon \; L^2(R)$. We denote P_j as the projection operator onto the space V_j. We define the *scaling function coefficient* as $s_k^j = (f, \tilde{\phi}_k^j)$. Similarly let Q_j be the projection operator onto W_j. We define the *wavelet coefficient* as $d_m^j = (f, \tilde{\psi}_m^j)$. Thus we have the following series representation:

$$P_j f(x) = \sum_{k \varepsilon \mathbb{K}(j)} s_k^j \phi_k^j \qquad Q_j f(x) = \sum_{m \varepsilon \mathbb{M}(j)} d_m^j \psi_m^j$$

For computational purposes spatial localization is extremely important, as it directly influences the computational stencil, which in turn dominates parallel performance. Thus we utilize the SGW basis functions element wise in a DG-SEM discretisation. Thus a signal over the elements may be represented as:

$$f(x) \simeq P_J f(x) = \sum_{\mathbb{T}} \Big(\sum_k s_k^0 \phi_k^0 + \sum_{j=0}^{J-1} \sum_m d_m^j \psi_m^j \Big)$$

Using this description of a function, we can now describe the adaptive algorithm based upon the wavelets. We begin by constructing a coarse approximation space with a given number of elements. During the course of the computation the flow variables are subjected to an MRA. The *scaling functions* serve as low-pass filters while the *wavelets* serve as high-pass filters. Thus we examine the magnitude of the *wavelet coefficients* and compare them to a predefined *threshold* (ε). In the smooth regions of the flow the wavelet coefficients are predominantly zero. A proliferation of wavelet coefficients exceeding the threshold, in any region of the flow, indicates the presence of structures that contributes to the high frequencies in a spectral analysis and thus to the numerical errors. To resolve these regions better, mesh refinement is performed locally. It should be noted that this refinement indicator is completely

Fig. 1 Streamline pattern

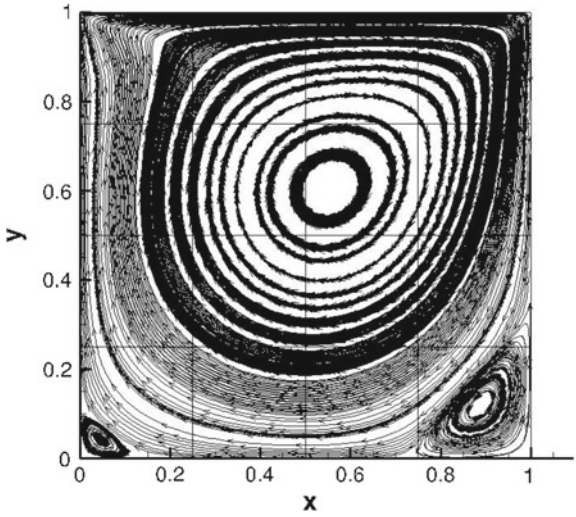

blind to sudden jumps across the *interfaces* which is fortuitous as DG-SEM by its very nature produces a discontinuous solution across elements.

4 Numerical Test

The method proposed above has been implemented into an unstructured code for 2D and 3D. It has been written in C++ and uses MPI for parallel multi-domain calculations. We demonstrate the method via a classic test case—the lid driven cavity problem at $Re = 400$. DNS data for this test case is available in [10]. We perform a DG-SEM calculation on a domain discretized with 4×4 elements, with Q_8–Q_8 discontinuous velocity-pressure approximation space per element, providing a total of $1,296$ degrees of freedom (G1) (Fig. 2). We then perform a single cycle of h-adaptivity based upon the MRA of the u component of the velocity to produce a geometrically non-conforming grid (G2) (Fig. 2) with $3,969$ degrees of freedom.

For comparison we extract the u and v velocities along the vertical and horizontal center-lines and compute the vorticity (ω_z) along the moving wall for grids G1 and G2. These quantities are compared with the reference data. The curves in Fig. 3 clearly illustrated the benefit of the wavelet adapted grid. We see that although the u and v velocity predictions exhibit a negligible improvement the ω_z prediction has improved dramatically particularly in the region $0 \leq x \leq 0.3$. Although this test case is extremely mild it serves to demonstrate the method in its entirety and demonstrates how adaptivity may be performed in incompressible flows cheaply and effectively.

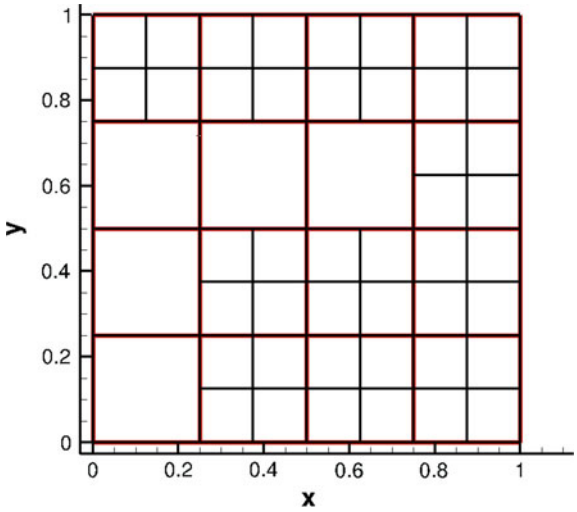

Fig. 2 G1 in *red*, G2 in *black*

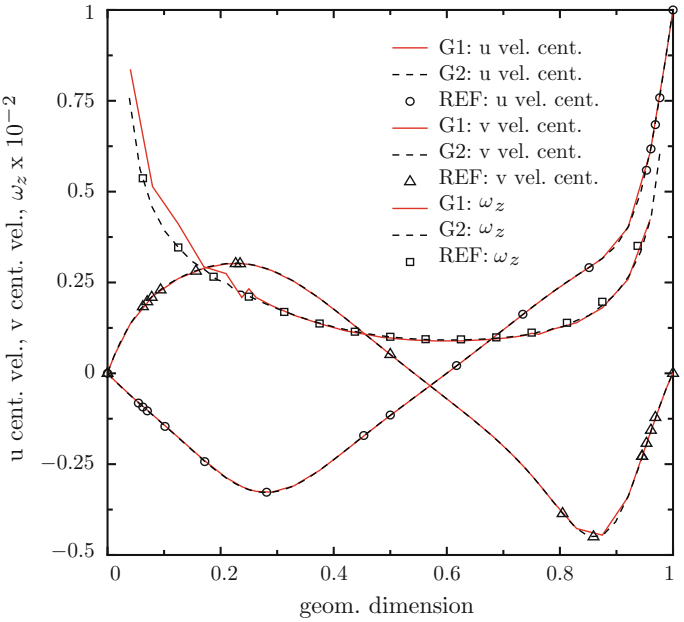

Fig. 3 Comparison of *centreline* velocity (u, v) and moving wall vorticity ω_z

5 Conclusions

We have outlined the development of a wavelet based adaptive DG-SEM scheme for incompressible flows. The usage of DG-SEM in conjunction with the SGW appears to have a number of advantages which we have demonstrated via the lid driven cavity test case. The overall strategy is fairly unique and should prove useful for unsteady detached flows for which error estimators and refinement indicators are severely lacking. However work must be done in determining the flow variables upon which the MRA should be performed as well as the appropriate choice of the threshold. In the near future we hope to extend our approach to more challenging turbulent flow problems such as the prediction of the skin-friction coefficient in the recirculation region of the backward-facing step.

Acknowledgements This work was funded by ONERA. I would like to express my sincere thanks to Vincent Couaillier for his help during the course of this work.

References

1. George EM (2004) Karniadakis and spencer sherwin, spectral/hp element method for computational fluid dynamics. Oxford Science Publications
2. Ern A, Di Pietro D (2010) Mathematical aspects of discontinuous Galerkin methods. Springer, Heidelberg
3. Chapelier J-B, De La Llave Plata M, Renac F, Lamballais E (2014) Evaluation of a high-order discontinuous Galerkin method for the DNS of turbulent flows. Comput Fluids 95(22): 210226
4. Schneider K, Vasilyev OV (2010) Wavelet methods in computational fluid dynamics. Annu Rev Fluid Mech 42:473–503
5. Gerhard N, Iacono F, May G, Muller S, Schafer R (2015) A high-order discontinuous Galerkin discretisation with multiwavelet-based grid adaptation for compressible flows. J Scient Comput
6. Cockburn B, Kanschat G, Schötzau D (2009) An equal-order DG method for the incompressible Navier–Stokes equations. J Scient Comput 40:188–210
7. Shahbazi K, Fischer PF, Ethier CR (2007) A high-order discontinuous Galerkin method for the unsteady incompressible Navier–Stokes equations. J Comput Phys 222:391–407
8. Guermond JL, Minev P, Shen J (2006) An overview of projection methods for incompressible flow. Compu Methods Appl Mech Eng 195:6011–6045
9. Sweldens W, Schröder P (1995) Building your own wavelets at home, Industrial Mathematics Initiative, Department of Mathematics, University of South Carolina, Technical Report 1995:5
10. Ghia U, Ghia KN, Shin CT (1982) High-Re solutions for incompressible flow using the Navier–Stokes equations and a multigrid method. J Comput Phys 48:387–411